Matrix Biology 38 (2014) 3–11

Contents lists available at ScienceDirect

Matrix Biology

journal homepage: www.elsevier.com/locate/matbio

Assessment of hyaline cartilage matrix composition using near infrared spectroscopy

Uday P. Palukuru, Cushla M. McGoverin, Nancy Pleshko *

Department of Bioengineering, Temple University, 1947 N. 12th St, Philadelphia, PA, USA

ARTICLE INFO

Article history:
Received 1 March 2014
Received in revised form 18 July 2014
Accepted 19 July 2014
Available online 29 July 2014

Keywords:
Near infrared spectroscopy
Articular cartilage
Partial least square regression
Collagen
Chondroitin sulfate

ABSTRACT

Changes in the composition of the extracellular matrix (ECM) are characteristic of injury or disease in cartilage tissue. Various imaging modalities and biochemical techniques have been used to assess the changes in cartilage tissue but lack adequate sensitivity, or in the case of biochemical techniques, result in destruction of the sample. Fourier transform near infrared (FT-NIR) spectroscopy has shown promise for the study of cartilage composition. In the current study NIR spectroscopy was used to identify the contributions of individual components of cartilage in the NIR spectra by assessment of the major cartilage components, collagen and chondroitin sulfate, in pure component mixtures. The NIR spectra were obtained using homogenous pellets made by dilution with potassium bromide. A partial least squares (PLS) model was calculated to predict composition in bovine cartilage samples. Characteristic absorbance peaks between 4000 and 5000 cm^{-1} could be attributed to components of cartilage, i.e. collagen and chondroitin sulfate. Prediction of the amount of collagen and chondroitin sulfate in tissues was possible within 8% (w/dw) of values obtained by gold standard biochemical assessment. These results support the use of NIR spectroscopy for in vitro and in vivo applications to assess matrix composition of cartilage tissues, especially when tissue destruction should be avoided.

1. Introduction

Articular cartilage is a type of hyaline cartilage found on the articular surfaces of bones in diarthrodial joints and functions to provide a near frictionless and load bearing surface to facilitate smooth joint movement. This tissue is hypocellular, avascular, aneural, alymphatic and contains only one type of differentiated cell, chondrocytes, which maintain the extra cellular matrix (ECM) (Fox et al., 2009). The functionality of articular cartilage is inherently linked to chemical composition. The ECM of articular cartilage is primarily composed of collagen type II fibrils (15–25% wet weight), proteoglycans (PG) (5–10% wet weight) and water (70–80% wet weight) (Cohen et al., 1998). Mature articular cartilage displays a zonal architecture with varied chemical composition, collagen fibril orientation and chondrocyte shape in the superficial, transitional, and deep zones (Buckwalter et al., 1994).

Injury or disease [e.g. osteoarthritis (OA)] in articular cartilage may cause the degradation of ECM structure and inhibit function; subsequently, joint pain and a loss in mobility may occur. Degenerative changes in ECM include the disruption of collagen fibrils which restricts PG water binding capacity and leads to swelling. The changes in collagen and PG content play an important factor in disease progression and need to be evaluated accurately for the development of successful intervention strategies. Several modalities are utilized to evaluate the composition of cartilage including optical arthroscopy, computed tomography (CT) based arthrography and magnetic resonance imaging (MRI) for *in vivo* studies (Hayes and Conway, 1992; Chung et al., 2001; Cockman et al., 2006; Domayer et al., 2008; Piscaer et al., 2008; Roemer et al., 2009; Siebelt et al., 2011b). MRI has been used extensively to evaluate the morphology and composition of osteoarthritic tissue non-invasively but has inadequate specificity and sensitivity at a molecular level, is expensive, and cannot be used intra-operatively (Gelb et al., 1996; Nishii et al., 2005; Lin et al., 2009a,b; Sutter et al., 2014). CT has also been used extensively to evaluate morphology of osteoarthritic tissue non-invasively but suffers from lack of sensitivity, has the added disadvantage of incorporating ionizing radiation, and also is not used intra-operatively (Daenen et al., 1998; Rand et al., 2000; Bansal et al., 2011; Siebelt et al., 2011a).

Infrared (IR) spectroscopy is a technique based on the interactions between infrared radiation and matter that enables molecular characterization of samples (Siebert, 1995). The chemical bonds within molecules of a sample have unique vibrational frequencies and infrared wavelengths incident on a sample that resonant with these frequencies are absorbed. This allows the molecular characterization of a sample as each molecule has a unique absorption profile across the infrared spectral range. Fourier transform infrared (FTIR) spectroscopy has been used to investigate the chemical composition of many biological tissues including cartilage in both the mid infrared (MIR) spectral range (4000–400 cm^{-1}) (Camacho et al., 2001; Potter et al., 2001; Kim et al.,

* Corresponding author at: Department of Bioengineering, Temple University, 1947 N. 12th St, Rm 839, Philadelphia, PA 19122, USA. Tel.: +1 2152044280.
E-mail address: npleshko@temple.edu (N. Pleshko).

http://dx.doi.org/10.1016/j.matbio.2014.07.007
0945-053X/

2005; Krafft and Sergo, 2006; Boskey and Pleshko Camacho, 2007; Xia et al., 2007; Movasaghi et al., 2008; Rieppo et al., 2012b) and near infrared (NIR) spectral range (10,000–4000 cm^{-1}) (Brown et al., 2009; Baykal et al., 2010; Afara et al., 2012; Padalkar et al., 2013). Studies have been performed in the MIR region to assess the spectral signatures of the pure components present within the cartilage matrix (Camacho et al., 2001; Potter et al., 2001). An infrared fiber optic probe (IFOP) coupled to an FTIR spectrometer may be used to collect spectra directly from the surface of an intact sample using attenuated total reflectance in the MIR region; this method has shown promise for clinical studies (West et al., 2004; Li et al., 2005; Hanifi et al., 2013). However, the MIR region has limited penetration depth (up to 10 μm maximum); hence, these studies incorporate information from only the first few micrometers of the tissue. For greater penetration depth, NIR spectroscopy is superior. However, the absorbances in NIR spectra are very low, and generally arise from a combination of molecular species, making assignments of specific peaks challenging. Nevertheless, several studies have demonstrated the effectiveness of NIR spectroscopy in evaluating cartilage tissue quality non-destructively (Spahn et al., 2007, 2008; Brown et al., 2009; Baykal et al., 2010; Afara et al., 2012, 2013a, 2013b, 2013c; Padalkar et al., 2013). Studies have also shown that the NIR spectra obtained using an IFOP can be used to monitor disease progression in OA cartilage, and that this modality can perform better than other clinically used procedures to evaluate cartilage degeneration (Hofmann et al., 2010; Brown et al., 2011, 2012; Spahn et al., 2013b). Most of these studies are focused on regions of the NIR spectra that are based on water absorbance and where cartilage tissue component contributions highly overlap. Many of these studies have also focused on using NIR spectra for evaluation of tissue composition without attributing specific absorbances in NIR spectra to individual tissue components, other than water. Knowledge of specific absorbance peak assignments in the NIR spectral region would enable increased understanding of these complicated spectra.

Problems associated with NIR spectroscopy, including signal overlap, can be overcome by using multivariate data analysis techniques [for example principal component analysis (PCA) and partial least square regression (PLS-R) coupled with signal preprocessing techniques e.g. extended multiplicative scatter correction (EMSC) and second derivatives]. The multivariate techniques PCA and PLS-R were used to successfully to evaluate cartilage tissue and pure components of cartilage in the MIR region (Yin and Xia, 2010; Hanifi et al., 2012; Rieppo et al., 2012a). In work by Padalkar et al. (2013) the composition of water in hyaline cartilage was evaluated quantitatively using NIR spectroscopy, but the study did not evaluate cartilage pure matrix components.

There are two primary goals of the current study: 1) identify the contributions of individual matrix components of cartilage to absorbances in the NIR spectral range and 2) demonstrate the feasibility of NIR spectroscopy for quantitative compositional assessment of cartilage. Cartilage pure components, namely collagen and chondroitin sulfate (which is a major component of proteoglycans), were mixed in various ratios and NIR spectra collected. Pure component mixture NIR spectra and multivariate techniques were used to predict the composition of bovine articular and nasal cartilage from their corresponding NIR spectra, and these predictions were compared to gold standard biochemistry measurements. Collectively these studies demonstrate that NIR spectroscopy can be used to quantitatively, and non-destructively, evaluate the composition of cartilage tissue.

2. Results

2.1. NIR spectral analysis of KBr pellets

The NIR spectra of multicomponent samples often contain broad features due to overlap of contributions from individual components. This is clearly evident in the scatter corrected and normalized spectra of the collagen and chondroitin sulfate mixtures [Fig. 1a]. Bands centered at ~4610 and 4890 cm^{-1} are observed to increase in intensity with increasing collagen content in the scatter corrected and normalized spectra. However, no readily discernible peaks that can be attributed to increasing chondroitin sulfate content are observable. Second derivative processing revealed additional features of the data. With increasing collagen content, peaks centered near 4050 and 4260 cm^{-1} appeared, and similarly, peaks centered near ~4020 and 4310 cm^{-1} increased in intensity with increasing chondroitin sulfate content [Fig. 1b, (Note: second derivative peaks are negative)]. The second derivative NIR spectra of biological samples (young and adult articular cartilage, and adult nasal cartilage) supported these absorbance band assignments [Fig. 2]. Collagen peaks were most intense in young and adult articular cartilage, and were least intense in nasal cartilage, as was expected from a literature assessment of collagen content within these tissue types.(Goh and Lowther, 1966; Campo and Tourtellotte, 1967; Eyre and Muir, 1975; Heinegard and Paulsson, 1987).

2.2. Biochemical assessment of powders

The collagen content of young articular cartilage, adult articular cartilage, and young nasal cartilage was assessed by measuring the amount of hydroxyproline present in the samples [Table 1]. Hydroxyproline which is one of the three major amino acids present in the collagen protein chain is frequently used to estimate the total collagen content in samples (Hosseininia et al., 2013; McAlinden et al., 2014). The amount of collagen in the cartilage powders averaged 72.9% weight/dry weight (w/dw) in adult articular cartilage, 64.1% w/dw in young articular cartilage and 41.5% w/dw in nasal cartilage. Among the cartilage powders the amount of sulfated glycosaminoglycans (sGAG) varied from an average of 19.7% w/dw in adult articular cartilage to 52.7% w/dw in nasal cartilage [Table 1].

2.3. Prediction of major cartilage components using NIR spectral data

A partial least squares (PLS) model was calculated from the pure component mixture spectra for collagen and chondroitin sulfate content; the root mean square error of prediction (RMSEP) was 8% w/dw and R^2 was 0.95 [Fig. 3]. The loading weights of the factors used in the PLS model incorporated the unique spectral features attributed to the individual components [Fig. 4]. Unsurprisingly, features characteristic to collagen and chondroitin sulfate were present predominantly in the loading weights of the first factor, which accounted for nearly 90% of variation in the samples. The PLS model predicted the highest percentage of collagen in adult articular cartilage, followed by young articular cartilage, and then nasal cartilage powder [Table 1]. Chondroitin sulfate content as predicted by the PLS model followed the reverse trend [Table 1].

3. Discussion

To more effectively use NIR spectroscopy to assess changes in the ECM of biological tissues such as hyaline cartilage, it is important to understand the NIR spectral signatures of the individual components of the tissue matrix. The use of sample powders diluted with a NIR transmissive salt to extract NIR signatures is a standard practice, and was employed in this work to observe the NIR spectra of pure cartilage ECM components. NIR spectra of collagen and chondroitin sulfate mixtures had differences which were attributed to the individual components, in particular when the second derivative spectra were examined. These spectral differences were also present in cartilage powders of varying biochemical composition [Figs. 1b and 2b]. Although there are no previous studies available on the specific interpretation of the NIR spectra of cartilage, NIR studies of agricultural and meat products with similar components (proteins and sugars) identified absorbance peaks attributable to protein, and cellulose and starch, two biopolymers with high sugar content (Osborne and Douglas, 1981; Weyer, 1985;

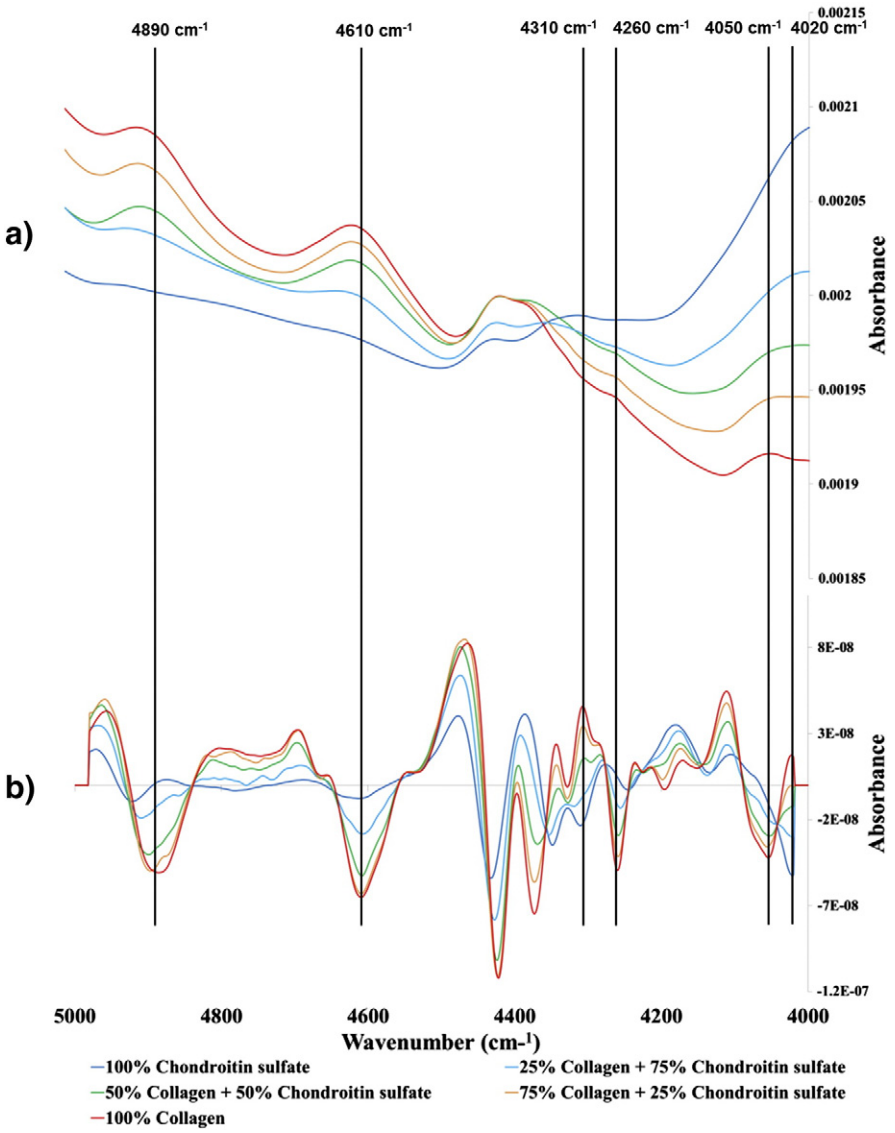

Fig. 1. The average scatter corrected and normalized (a) and second derivative spectra (b) of KBr pellet mixtures of collagen and chondroitin sulfate. Vertical lines indicate peaks of interest.

Rodriguez-Saona et al., 2001; Shenk et al., 2001; Alomar et al., 2003). The peak at 4050 cm^{-1} [Fig. 1b] was shown to arise from a C – H combination and symmetric first overtone of the C – N – C stretch of protein molecules. The CH_2 bond bending vibration and second overtone is also present in proteins and contributes to the peak at 4260 cm^{-1}. The asymmetric C – H stretch and C – H deformation combination contributes to the peak at 4610 cm^{-1}, whereas the N – H in-plane bending vibration contributes to the peak at 4890 cm^{-1} in proteins. Similarly, the C – H stretch and C – C stretch combination contributes to the peak at 4020 cm^{-1} in cellulose, and the C – H stretch and CH_2 deformation vibration combination contributes to the peak at 4310 cm^{-1} in starch. As cartilage contains no cellulose or starch, the peaks at 4020 and 4310 cm^{-1} can be attributed to the sugar component of proteoglycans. Similarly the peaks at 4050, 4260, 4610 and 4890 cm^{-1} can be attributed to collagen content as the majority of protein in cartilage is collagen. A peak at 4350 cm^{-1} apparent in samples with high chondroitin sulfate content merges with the peak at 4375 cm^{-1} in tissue samples, and along with the peak at 4420 cm^{-1} is indicative of the total protein and sugar content in the cartilage samples. The peaks at 4260, 4610 and 4890 cm^{-1}, although indicative of collagen content in tissue, cannot be used individually to differentiate tissue types with high protein content due to spectral overlap [Fig. 2b], clearly indicating the need for use of multivariate analysis.

In addition to identification of specific NIR peaks that arise from collagen and chondroitin sulfate, the current study also demonstrates that NIR spectral data can predict the percentage of collagen and chondroitin sulfate in a given biological sample with a reasonable prediction error. The PLS model predicted collagen and chondroitin sulfate content of samples to within 8% of values obtained by biochemical assessment. Previous studies have incorporated the contribution of water in cartilage sample assessment (Spahn et al., 2007, 2008; Brown et al., 2009; Baykal et al., 2010; Afara et al., 2012, 2013a, 2013b; Padalkar et al., 2013; Spahn et al., 2013a); this was not addressed in this study as the absorption bands of water have higher signal intensity and often overwhelm the contributions from the other components of cartilage tissue. Thus, the goal here was to utilize a spectral range with limited water contribution. The effect of water will be reduced in in vivo NIR spectral measurements if the NIR spectral acquisition is limited to 4000–5000 cm^{-1}, as the nearest broad absorption band attributable to water starts above 5000 cm^{-1} (Padalkar et al., 2013). The study by Padalkar et al. (2013) also found that water content varies greatly with the extent of time tissues are exposed to the atmosphere, and results in varied data

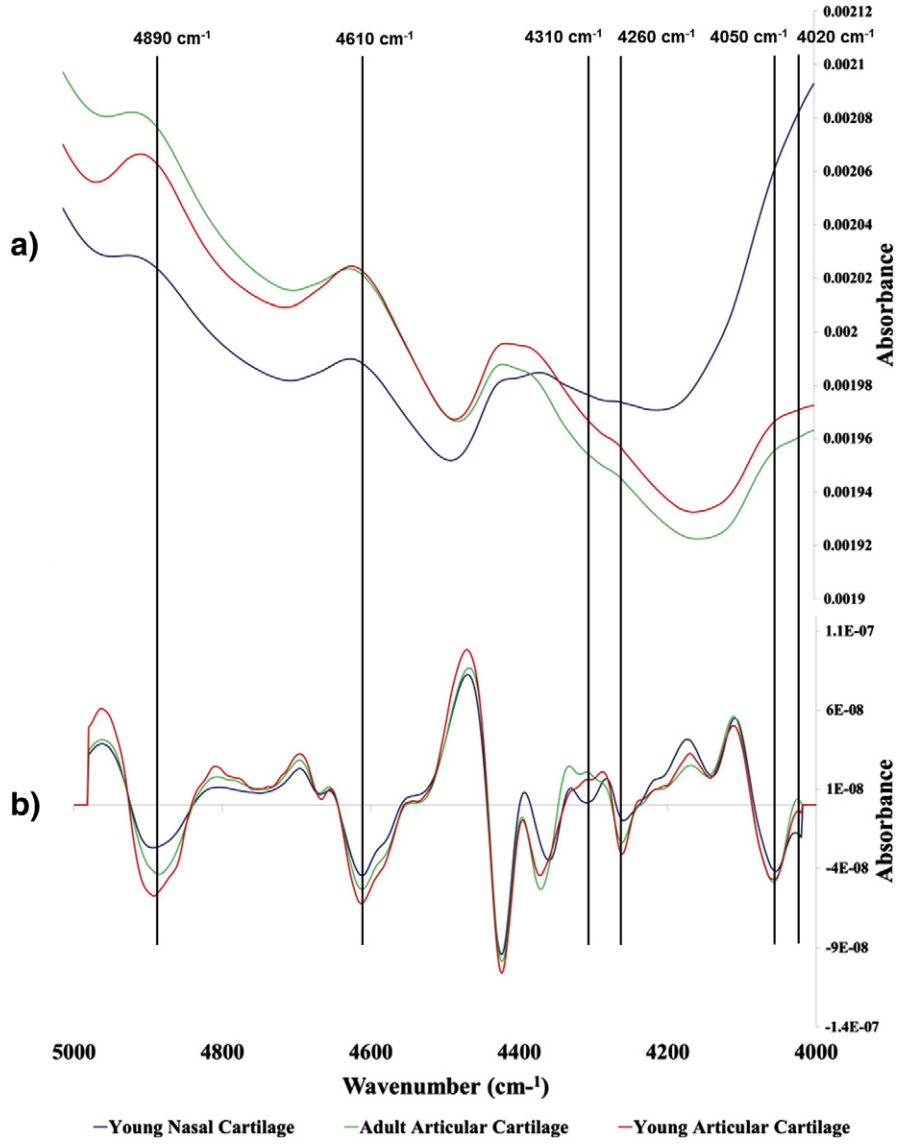

Fig. 2. The average scatter corrected (a) and second derivative spectra (b) of articular cartilage and nasal cartilage powders. Vertical lines indicate peaks of interest.

interpretation, further justifying investigation of a reduced spectral range.

Collagen is predominantly type II in articular cartilage and type I in bone, and a study in the mid infrared spectral range has discriminated type I and type II collagen within tissue using multivariate analysis (Hanifi et al., 2013). As the absorbances in the NIR spectral range are combinations of fundamental vibrations that arise from the various molecular bonds of component molecules, the differences between type I and type II collagen spectra are not readily discernible [Fig. 5]. Differences are present in the region near ~4310 cm^{-1}, and are likely due to a difference in glycosylation of the collagen molecules (Brodsky and Eikenberry, 1985; van der Rest and Garrone, 1991). Nonetheless, the use of collagen type I rather than collagen type II (which was done due to the greater availability of type I collagen in the quantities required for this study) is not considered a significant source of error within the model. The hydroxyproline method used to assess collagen content in tissues and powders also cannot distinguish between type I and type II collagen as both types contain approximately the same

Table 1
The percentages of collagen and chondroitin sulfate (w/dw) present in nasal and articular cartilage powders as predicted by the NIR PLS model, and as determined from biochemical analyses.

Powder type	Number of KBr pellets used for NIR data	Collagen % w/dw prediction based on NIR data (SD)	Chondroitin sulfate % w/dw prediction based on NIR data (SD)	Number of samples used for biochemical analysis	Collagen % w/dw based on biochemical data (SD)	Chondroitin sulfate % w/dw based on biochemical data (SD)
Young nasal cartilage	5	51.5 (±0.67)	48.5 (±0.67)	3	41.5 (±2.5)	52.7 (±4.1)
Young articular cartilage	5	72.7 (±0.97)	27.3 (±0.97)	3	64.1 (±2.2)	34.6 (±1.9)
Adult articular cartilage	5	78.4 (±0.65)	21.6 (±0.65)	3	72.9 (±0.1)	19.7 (±0.0)

[SD] indicates standard deviation.

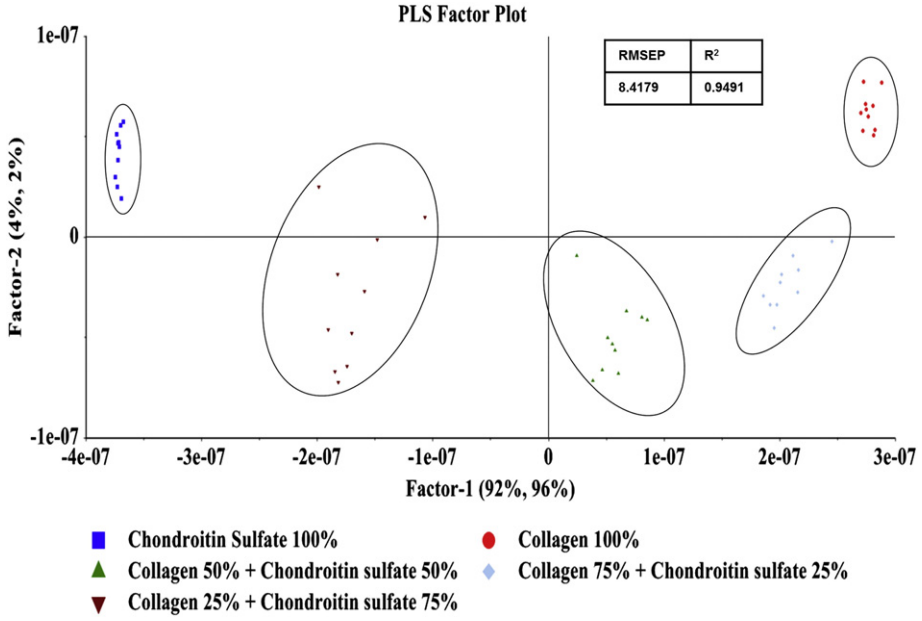

Fig. 3. The first versus second factor plot of the PLS model of collagen and chondroitin sulfate KBr pellet mixtures illustrating the pellet sample groupings based on varying collagen percentages.

percentage of hydroxyproline (Click and Bornstein, 1970; Miller and Lunde, 1973).

The NIR spectra of proteins have also been shown to contain information regarding secondary structure (Miyazawa and Sonoyama, 1998; Robert et al., 1999). Serum albumin is a major component of blood and has been extensively characterized using NIR spectroscopy. The NIR spectrum of bovine serum albumin (BSA) [Fig. 5] is dominated by spectral features attributed to the alpha-helical structures found

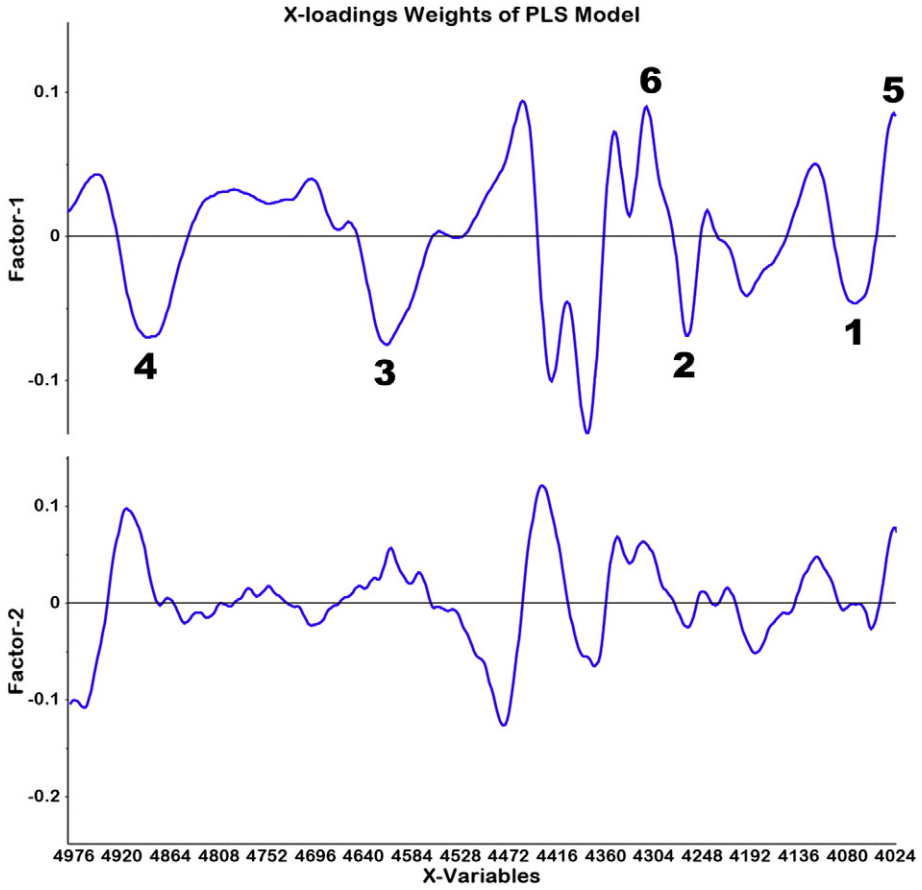

Fig. 4. The weights for the X-loadings used in the PLS model for estimation of collagen in pellet samples. Peaks of interest related to pure collagen spectrum (1–4) and chondroitin sulfate (5–6). Since a binary system was used for building the PLS model, the loadings for estimation of chondroitin sulfate percentage are inverse and hence not shown.

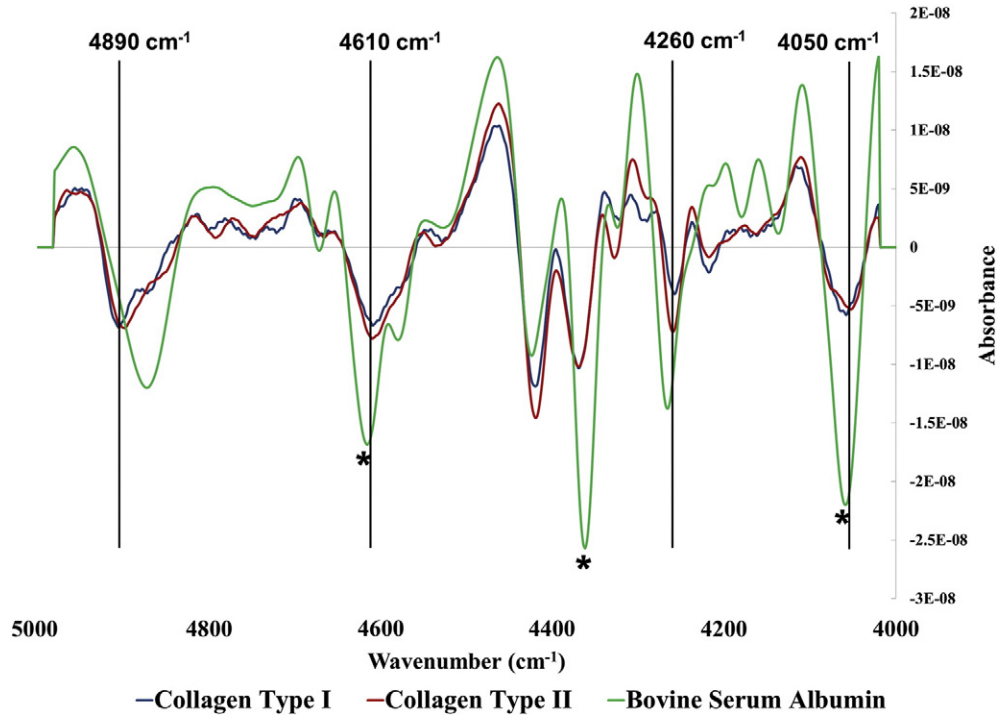

Fig. 5. The average second derivative spectra of collagen (types I and II) and bovine serum albumin (BSA). Absorbances were not fully normalized between the BSA and collagens to permit distinction in peak absorbances. Vertical lines indicate peaks of interest in collagen samples. * indicate peaks attributed to alpha-helical structures of albumin. In collagen samples the differences in the region between 4260 and 4400 cm^{-1} likely arise from glycosylation differences.

within the protein (Izutsu et al., 2006). These peaks, particularly 4090, 4370 and 4615 cm^{-1} were shifted or of lower intensity in the collagen spectra. Collagen proteins are devoid of alpha-helical structures and display only a triple helical structure, hence the observed peak differences. Thus, there are differences in the spectral features of albumin and collagens that could be especially important in a clinical context, as significant injury to cartilage has been shown to cause rupture of underlying blood vessels and release of blood.

Proteoglycans in the cartilage matrix are predominantly composed of chondroitin sulfate and keratin sulfate GAG chains attached to the hyaluronic acid backbone via a link protein. The ratio of chondroitin sulfate and keratin sulfate in hyaline cartilage has been estimated to be 2:1 with chondroitin sulfate being 4 times heavier than keratin sulfate (Hardingham, 1981). Thus, the use of chondroitin sulfate as a proxy for proteoglycan content was acceptable and has also been used to reflect proteoglycan content in other compositional studies (Potter et al., 2001; Williamson et al., 2001; Nieminen et al., 2002). Further, in spite of the relatively greater amount of protein compared to sGAG content in the cartilage samples the unique absorbance bands at 4310 and 4020 cm^{-1} were still present, which were attributed to the sugar rings found in sGAG and in PGs.

Chondrocytes are important for the health of cartilage but account for a small volume of the cartilage matrix. Thus, the absorbances in the NIR region from the intracellular components of chondrocytes, primarily lipids and nucleic acids, would have very low intensity, and would overlap with the absorption bands from proteins and sugars. The PLS model used in these studies was based only on the contributions of collagen and chondroitin sulfate, while the contributions from intracellular components (and water) were not considered. Nonetheless, it is possible that the errors observed in the model (~8% w/dw) could be attributed to non-collagen and non-chondroitin sulfate components, including lipids and nucleic acids, and other collagen types that are present in small amounts in cartilage.

Many of the previous NIR spectroscopic studies of cartilage have focused on characterizing tissue using water absorbances (10,200, 8100, 7000, 5200 cm^{-1}) and tissue matrix absorbances above 6200 cm^{-1} (Oluwaseun et al., 2011; Spahn et al., 2013a). Although these studies were successful in characterizing the quality of the tissue, the overlap from combination bands and water absorbances did not permit the identification of the source of the matrix bands. A recent study from our lab used the extended NIR range of 3800–5400 cm^{-1} and first derivative spectra to study collagen and proteoglycan concentration of engineered cartilage tissue, but individual matrix combinations were not identified (Baykal et al., 2010). In the current study peaks recognized as arising from individual matrix components were clearly distinguished using a narrow range of 4000–5000 cm^{-1} and second derivative spectra. Even with the use of second derivative spectra, the use of multivariate data analysis techniques was required to clearly elucidate the differences in the spectra with increasing concentrations of components.

Various hydroxyproline and sGAG biochemical studies have shown differences in collagen and proteoglycan content of cartilage tissue of varying age and location (Hoemann, 2004). However the accuracy of these methods varies by investigators and the method used, which is of great importance as these are the methods considered to be “gold standards” for estimation of cartilage tissue composition. Thus, the error in our gold standard method for comparison to PLS may be comparable to the error in model developed. The RMSEP of the PLS model in this study was 8% w/dw; a previous MIR based PLS model had a RMSEP of 4% w/dw (Hanifi et al., 2013). The lower error of prediction in the MIR model can possibly be attributed to better defined absorption peaks in MIR arising from primary absorbances, versus broad and overlapping peaks in NIR arising from overtones and combinations of the primary absorbances. Another source of error in the NIR model may result from non-uniform mixing of powders when preparing the pellet samples. Non-uniform mixing of powder mixtures has been reported in industrial scale mixing methods and is expected in pellet mixtures made by hand (Bridgwater, 1976; Venables and Wells, 2001). In spite of the prediction error in the PLS model, the technique can be used for qualitative assessment of tissue composition, or if seeking to evaluate differences that are larger than the model error. Disease and aging

induced changes in cartilage tissue composition ranging from 20% collagen w/dw to 12% total sGAG content w/dw have been reported in literature (Matthews, 1953; Bollet et al., 1963; Mankin and Lippiell, 1971a,b; Venn and Maroudas, 1977; Squires et al., 2003).

For in vivo assessment of cartilage composition, a NIR fiber optic probe can be combined with PLS regression analysis to semi-quantitatively assess the composition of cartilage tissue, and thereby complement existing arthroscopic and radiographic techniques. Similarly, such a system can be used in vitro to reduce the number of samples required for assessment of cartilage composition, especially in tissue engineering applications, where sample numbers can be limited. To move toward in vivo evaluation of component molecules using NIR spectroscopy, future studies are required where modeling parameters are applied to NIR fiber optic data obtained from varying sources of cartilage, including during clinical procedures.

In summary, the current study has identified unique NIR spectral features that arise from pure components of cartilage and demonstrated the use of multivariate analysis to predict the percentage of collagen and chondroitin sulfate in tissue samples. The results indicate that this spectroscopic method may be used in lieu of destructive biochemical sampling techniques when it is necessary to save the tissues of interest. The use of this NIR spectral region (4000–5000 cm^{-1}) to quantitate cartilage components requires further validation. Nevertheless, it has the potential to be applied in vivo and in vitro via an NIR fiber optic probe technique, where it could be used to assess tissue composition in real time for clinical or laboratory applications.

4. Experimental procedures

4.1. Materials

Bovine hide derived high purity collagen (primarily type I) was generously provided by DSM Biomedical (Exton, PA). Bovine high purity collagen type II purified from bovine articular cartilage was purchased from United States Biological Corporation (Swampscott, MA). Bovine cartilage derived chondroitin sulfate powder was purchased from Sigma Aldrich (St. Louis, MO), bovine serum albumin from Equitech-Bio Incorporated (Kerrville, TX) and potassium bromide (KBr) powder from Agilent Technologies (New Castle, DE). Adult (1–2 years) and young (3–6 weeks) bovine knee joints and snouts were obtained from Green Village Packing (Green Village, NJ) within 24 h of slaughter. These tissues were chosen as they were expected to exhibit a range of collagen and chondroitin sulfate composition. Articular and nasal cartilage plugs were extracted from cartilage surfaces using a 5 mm biopsy punch (Ted Pella, Redding, CA). Proteinase K powder, 1, 9-dimethyl methylene blue (DMMB) dye, 4-(dimethylamino) benzaldehyde (DMAB), sodium acetate trihydrate, 1-propanol, perchloric acid, tris–ethylenediamine tetraacetic acid (tris–EDTA) solution and cis-4-hydroxy-d-proline (Hyp) powder were purchased from Sigma Aldrich (ST. Louis, MO). Hydrochloric acid (HCl), citric acid monohydrate, glacial acetic acid, chloramine-T, tris–hydrochloride (Tris–HCl), calcium chloride ($CaCl_2$), sodium chloride (NaCl), sodium hydroxide (NaOH), glycine, ethanol and 96 well plates were purchased from Fisher Scientific (Fair Lawn, NJ).

4.2. Powders and pellet preparation

Cartilage plugs were weighed and lyophilized for 3 days. Collagen, albumin and cartilage fine powders were prepared by freeze milling using a Freezer Mill 6770 from SPEX Sample Prep (Metuchen, NJ). The powders were subsequently lyophilized for an additional 2 days. Twenty milligram mixtures of collagen and chondroitin sulfate powders at varying concentrations (0, 25%, 50%, 75% and 100% collagen, with the remainder chondroitin sulfate) were mixed with 380 mg of KBr powder and pelleted under high pressure to obtain a 13 mm diameter pellet using a pellet press (Carver, Wabash, IN). The powder mixtures of pure components were mixed in bulk before being aliquoted for dilution with KBr powder; this was done to minimize losses due to mixing of small quantities of powders and to ensure uniform mixing. Similarly 20 mg of young and adult articular cartilage, and young nasal cartilage powders were prepared as pellets.

4.3. Biochemical assessment

Cartilage powders were digested for 18–24 h at 60°C using a Tris–HCl buffer solution containing 50 mM Tris–HCl, 1 mM $CaCl_2$ and proteinase K at 34 units per ml for every mg of dry powder at pH 8.0. The digests were then used to determine sGAG and hydroxyproline content in the powders by the dimethyl methylene blue (DMMB) and hydroxyproline assays, respectively (Farndale et al., 1986; Hoemann, 2004). Three 20 mg samples from cartilage powders were analyzed by DMMB and hydroxyproline assay with triplicate measurements by absorption at 525 and 550 nm, respectively using Infinite Pro 200 plate reader from Tecan (Crailsheim, Germany).

4.4. NIR data collection and processing

NIR spectral data from the pellets were collected using a Spectrum 400 spectrometer (Perkin Elmer, Waltham, MA). The range of 4000–5000 cm^{-1} was used for data collection to minimize the interference of the water absorption band at ~5200 cm^{-1} (Padalkar et al., 2013). The pellets were positioned in the beam path of the spectrometer at a slight angle in order to reduce the interference patterns (fringes) that result from total internal reflection. The spectral data resolution was 8 cm^{-1} and 512 scans were co-added. Data from 10 pellets were collected for each of the collagen and chondroitin sulfate mixtures, and from 5 pellets for cartilage powders. The scattering effect due to different particle sizes in the pellets was minimized by applying an extended multiplicative scatter correction to the raw spectral data. The scatter corrected spectra were then area normalized and converted to second derivative spectra by using a Savitzky Golay differentiation window of 84 cm^{-1} and 3rd order polynomial (Rieppo et al., 2012b). The second derivative of a curve is the rate of change of slope of the curve; this is useful for resolving overlapping peaks. The second derivative of a positive peak in the raw spectrum results in a negative peak, where the intensity of the second derivative peaks mirror the raw data peaks, but are more resolved. Principal least square (PLS) regression modeling was performed to predict the composition of pellets using the spectral data. The PLS model was validated using cross validation that included all spectra (n=10 per group, total of 50 spectra). However, a random collagen and chondroitin sulfate mixture group (10 spectra) were kept out of the calibration model for each iteration of the cross validation. The quality of the prediction model was evaluated based on the RMSEP, and the R^2 of actual vs. predicted values. The RMSEP of the model was calculated as:

$$\mathrm{RMSEP} = \sqrt{\frac{\Sigma(Yprediction(i) - Yexperiment(i))^2}{N}}$$

where i indicates the sample from 1 to N (Esbensen et al., 2002). Spectral preprocessing and statistical analysis were performed using The Unscrambler X from CAMO Software (Oslo, Norway).

Acknowledgments

This work was supported in part by NIH R01AR056145 and R01EB000744 grants. We would also like to thank DSM Biomedical for their generous donation of soluble collagen type I for this study.

References

Afara, I., Prasadam, I., Crawford, R., Xiao, Y., Oloyede, A., 2012. Non-destructive evaluation of articular cartilage defects using near-infrared (NIR) spectroscopy in osteoarthritic rat models and its direct relation to Mankin score. Osteoarthritis Cartilage 20, 1367–1373.

Afara, I., Singh, S., Oloyede, A., 2013a. Application of near infrared (NIR) spectroscopy for determining the thickness of articular cartilage. Med. Eng. Phys. 35, 88–95.

Afara, I.O., Prasadam, I., Crawford, R., Xiao, Y., Oloyede, A., 2013b. Near infrared (NIR) absorption spectra correlates with subchondral bone micro-CT parameters in osteoarthritic rat models. Bone 53, 350–357.

Afara, I.O., Singh, S., Oloyede, A., 2013c. Load-unloading response of intact and artificially degraded articular cartilage correlated with near infrared (NIR) absorption spectra. J. Mech. Behav. Biomed. Mater. 20, 249–258.

Alomar, D., Gallo, C., Castaneda, M., Fuchslocher, R., 2003. Chemical and discriminant analysis of bovine meat by near infrared reflectance spectroscopy (NIRS). Meat Sci. 63, 441–450.

Bansal, P.N., Joshi, N.S., Entezari, V., Malone, B.C., Stewart, R.C., Snyder, B.D., Grinstaff, M.W., 2011. Cationic contrast agents improve quantification of glycosaminoglycan (GAG) content by contrast enhanced CT imaging of cartilage. J. Orthop. Res. 29, 704–709.

Baykal, D., Irrechukwu, O., Lin, P.C., Fritton, K., Spencer, R.G., Pleshko, N., 2010. Nondestructive assessment of engineered cartilage constructs using near-infrared spectroscopy. Appl. Spectrosc. 64, 1160–1166.

Bollet, A.J., Handy, J.R., Sturgill, B.C., 1963. Chondroitin sulfate concentration and protein–polysaccharide composition of articular cartilage in osteoarthritis. J. Clin. Invest. 42, 853–859.

Boskey, A., Pleshko Camacho, N., 2007. FT-IR imaging of native and tissue-engineered bone and cartilage. Biomaterials 28, 2465–2478.

Bridgwater, J., 1976. Fundamental powder mixing mechanisms. Powder Technol. 15, 215–236.

Brodsky, B., Eikenberry, E., 1985. Supramolecular collagen assemblies. Ann. N. Y. Acad. Sci. 460, 73–84.

Brown, C.P., Bowden, J.C., Rintoul, L., Meder, R., Oloyede, A., Crawford, R.W., 2009. Diffuse reflectance near infrared spectroscopy can distinguish normal from enzymatically digested cartilage. Phys. Med. Biol. 54, 5579–5594.

Brown, C.P., Jayadev, C., Glyn-Jones, S., Carr, A.J., Murray, D.W., Price, A.J., Gill, H.S., 2011. Characterization of early stage cartilage degradation using diffuse reflectance near infrared spectroscopy. Phys. Med. Biol. 56, 2299–2307.

Brown, C.P., Oloyede, A., Crawford, R.W., Thomas, G.E., Price, A.J., Gill, H.S., 2012. Acoustic, mechanical and near-infrared profiling of osteoarthritic progression in bovine joints. Phys. Med. Biol. 57, 547–559.

Buckwalter, J.A., Mow, V.C., Ratcliffe, A., 1994. Restoration of injured or degenerated articular cartilage. J. Am. Acad. Orthop. Surg. 2, 192–201.

Camacho, N.P., West, P., Torzilli, P.A., Mendelsohn, R., 2001. FTIR microscopic imaging of collagen and proteoglycan in bovine cartilage. Biopolymers 62, 1–8.

Campo, R.D., Tourtellotte, C.D., 1967. The composition of bovine cartilage and bone. Biochim. Biophys. Acta 141, 614–624.

Chung, C.B., Frank, L.R., Resnick, D., 2001. Cartilage imaging techniques: current clinical applications and state of the art imaging. Clin. Orthop. Relat. Res. S370–S378.

Click, E.M., Bornstein, P., 1970. Isolation and characterization of the cyanogen bromide peptides from the alpha 1 and alpha 2 chains of human skin collagen. Biochemistry 9, 4699–4706.

Cockman, M.D., Blanton, C.A., Chmielewski, P.A., Dong, L., Dufresne, T.E., Hookfin, E.B., Karb, M.J., Liu, S., Wehmeyer, K.R., 2006. Quantitative imaging of proteoglycan in cartilage using a gadolinium probe and microCT. Osteoarthritis Cartilage 14, 210–214.

Cohen, N.P., Foster, R.J., Mow, V.C., 1998. Composition and dynamics of articular cartilage: structure, function, and maintaining healthy state. J. Orthop. Sports Phys. Ther. 28, 203–215.

Daenen, B.R., Ferrara, M.A., Marcelis, S., Dondelinger, R.F., 1998. Evaluation of patellar cartilage surface lesions: comparison of CT arthrography and fat-suppressed FLASH 3D MR imaging. Eur. Radiol. 8, 981–985.

Domayer, S.E., Welsch, G.H., Dorotka, R., Mamisch, T.C., Marlovits, S., Szomolanyi, P., Trattnig, S., 2008. MRI monitoring of cartilage repair in the knee: a review. Semin. Musculoskelet. Radiol. 12, 302–317.

Esbensen, K., Guyot, D., Westad, F., Houmoller, L.P., 2002. Multivariate data analysis-in practice: an introduction to multivariate data analysis and experimental design. Multivariate Data AnalysisCamo Process AS.

Eyre, D.R., Muir, H., 1975. The distribution of different molecular species of collagen in fibrous, elastic and hyaline cartilages of the pig. Biochem. J. 151, 595–602.

Farndale, R.W., Buttle, D.J., Barrett, A.J., 1986. Improved quantitation and discrimination of sulphated glycosaminoglycans by use of dimethylmethylene blue. Biochim. Biophys. Acta 883, 173–177.

Fox, A.J.S., Bedi, A., Rodeo, S.A., 2009. The basic science of articular cartilage: structure, composition, and function. Sports Health 1, 461–468.

Gelb, H.J., Glasgow, S.G., Sapega, A.A., Torg, J.S., 1996. Magnetic resonance imaging of knee disorders. Clinical value and cost-effectiveness in a sports medicine practice. Am. J. Sports Med. 24, 99–103.

Goh, A.T., Lowther, D.A., 1966. Effect of age on the composition of bovine nasal cartilage. Nature 210, 1270–1271.

Hanifi, A., Bi, X., Yang, X., Kavukcuoglu, B., Lin, P.C., DiCarlo, E., Spencer, R.G., Bostrom, M.P., Pleshko, N., 2012. Infrared fiber optic probe evaluation of degenerative cartilage correlates to histological grading. Am. J. Sports Med. 40, 2853–2861.

Hanifi, A., McCarthy, H., Roberts, S., Pleshko, N., 2013. Fourier transform infrared imaging and infrared fiber optic probe spectroscopy identify collagen type in connective tissues. PLoS One 8, e64822.

Hardingham, T., 1981. Proteoglycans: their structure, interactions and molecular organization in cartilage. Biochem. Soc. Trans. 9, 489–497.

Hayes, C.W., Conway, W.F., 1992. Evaluation of articular cartilage: radiographic and cross-sectional imaging techniques. Radiographics 12, 409–428.

Heinegard, D., Paulsson, M., 1987. Cartilage. Methods Enzymol. 145, 336–363.

Hoemann, C.D., 2004. Molecular and biochemical assays of cartilage components. Cartilage and OsteoarthritisSpringer, pp. 127–156.

Hofmann, G.O., Marticke, J., Grossstuck, R., Hoffmann, M., Lange, M., Plettenberg, H.K., Braunschweig, R., Schilling, O., Kaden, I., Spahn, G., 2010. Detection and evaluation of initial cartilage pathology in man: a comparison between MRT, arthroscopy and near-infrared spectroscopy (NIR) in their relation to initial knee pain. Pathophysiology 17, 1–8.

Hosseininia, S., Lindberg, L.R., Dahlberg, L.E., 2013. Cartilage collagen damage in hip osteoarthritis similar to that seen in knee osteoarthritis; a case–control study of relationship between collagen, glycosaminoglycan and cartilage swelling. BMC Musculoskelet. Disord. 14, 18.

Izutsu, K., Fujimaki, Y., Kuwabara, A., Hiyama, Y., Yomota, C., Aoyagi, N., 2006. Near-infrared analysis of protein secondary structure in aqueous solutions and freeze-dried solids. J. Pharm. Sci. 95, 781–789.

Kim, M., Bi, X., Horton, W.E., Spencer, R.G., Camacho, N.P., 2005. Fourier transform infrared imaging spectroscopic analysis of tissue engineered cartilage: histologic and biochemical correlations. J. Biomed. Opt. 10, 031105.

Krafft, C., Sergo, V., 2006. Biomedical applications of Raman and infrared spectroscopy to diagnose tissues. J. Spectro. 20, 195–218.

Li, G., Thomson, M., Dicarlo, E., Yang, X., Nestor, B., Bostrom, M.P., Camacho, N.P., 2005. A chemometric analysis for evaluation of early-stage cartilage degradation by infrared fiber-optic probe spectroscopy. Appl. Spectrosc. 59, 1527–1533.

Lin, P.C., Reiter, D.A., Spencer, R.G., 2009a. Classification of degraded cartilage through multiparametric MRI analysis. J. Magn. Reson. 201, 61–71.

Lin, P.C., Reiter, D.A., Spencer, R.G., 2009b. Sensitivity and specificity of univariate MRI analysis of experimentally degraded cartilage. Magn. Reson. Med. 62, 1311–1318.

Mankin, H.J., Lippiell, L., 1971a. Glycosaminoglycans of articular cartilage from aged normal and osteoarthritis human hip joints. J Bone Joint Surg Am A 53, 805-&.

Mankin, H.J., Lippiell, L., 1971b. Glycosaminoglycans of normal and arthritic cartilage. J. Clin. Investig. 50, 1712-&.

Matthews, B.F., 1953. Composition of articular cartilage in osteoarthritis; changes in collagen/chondroitin-sulphate ratio. Br. Med. J. 2, 660–661.

McAlinden, A., Traeger, G., Hansen, U., Weis, M.A., Ravindran, S., Wirthlin, L., Eyre, D.R., Fernandes, R.J., 2014. Molecular properties and fibril ultrastructure of types II and XI collagens in cartilage of mice expressing exclusively the alpha1(IIA) collagen isoform. Matrix Biol. 34, 105–113.

Miller, E.J., Lunde, L.G., 1973. Isolation and characterization of the cyanogen bromide peptides from the alpha 1(II) chain of bovine and human cartilage collagen. Biochemistry 12, 3153–3159.

Miyazawa, M., Sonoyama, M., 1998. Second derivative near infrared studies on the structural characterisation of proteins. J. Near Infrared Spectrosc. 6, 253–257.

Movasaghi, Z., Rehman, S., ur Rehman, D.I., 2008. Fourier transform infrared (FTIR) spectroscopy of biological tissues. Appl. Spectrosc. Rev. 43, 134–179.

Nieminen, M.T., Rieppo, J., Silvennoinen, J., Toyras, J., Hakumaki, J.M., Hyttinen, M.M., Helminen, H.J., Jurvelin, J.S., 2002. Spatial assessment of articular cartilage proteoglycans with Gd-DTPA-enhanced T1 imaging. Magn. Reson. Med. 48, 640–648.

Nishii, T., Tanaka, H., Nakanishi, K., Sugano, N., Miki, H., Yoshikawa, H., 2005. Fat-suppressed 3D spoiled gradient-echo MRI and MDCT arthrography of articular cartilage in patients with hip dysplasia. AJ. Am. J. Roentgenol. 185, 379–385.

Oluwaseun, A.I., Zenon, P., Adekunle, O., 2011. Current state of the application of infrared optical methods for assessing articular cartilage. J. Mater. Sci. Eng. A 1, 892–898.

Osborne, B.G., Douglas, S., 1981. Measurement of the degree of starch damage in flour by near infrared reflectance analysis. J. Sci. Food Agric. 32, 328–332.

Padalkar, M.V., Spencer, R.G., Pleshko, N., 2013. Near infrared spectroscopic evaluation of water in hyaline cartilage. Ann. Biomed. Eng. 41, 2426–2436.

Piscaer, T.M., Waarsing, J.H., Kops, N., Pavljasevic, P., Verhaar, J.A., van Osch, G.J., Weinans, H., 2008. In vivo imaging of cartilage degeneration using microCT-arthrography. Osteoarthritis Cartilage 16, 1011–1017.

Potter, K., Kidder, L.H., Levin, I.W., Lewis, E.N., Spencer, R.G., 2001. Imaging of collagen and proteoglycan in cartilage sections using Fourier transform infrared spectral imaging. Arthritis Rheum. 44, 846–855.

Rand, T., Brossmann, J., Pedowitz, R., Ahn, J.M., Haghigi, P., Resnick, D., 2000. Analysis of patellar cartilage. Comparison of conventional MR imaging and MR and CT arthrography in cadavers. Acta Radiol. 41, 492–497.

Rieppo, L., Rieppo, J., Jurvelin, J.S., Saarakkala, S., 2012a. Fourier transform infrared spectroscopic imaging and multivariate regression for prediction of proteoglycan content of articular cartilage. PLoS One 7, e32344.

Rieppo, L., Saarakkala, S., Närhi, T., Helminen, H., Jurvelin, J., Rieppo, J., 2012b. Application of second derivative spectroscopy for increasing molecular specificity of fourier transform infrared spectroscopic imaging of articular cartilage. Osteoarthr. Cartil. 20, 451–459.

Robert, P., Devaux, M.F., Mouhous, N., Dufour, E., 1999. Monitoring the secondary structure of proteins by near-infrared spectroscopy. Appl. Spectrosc. 53, 226–232.

Rodriguez-Saona, L.E., Fry, F.S., McLaughlin, M.A., Calvey, E.M., 2001. Rapid analysis of sugars in fruit juices by FT-NIR spectroscopy. Carbohydr. Res. 336, 63–74.

Roemer, F.W., Eckstein, F., Guermazi, A., 2009. Magnetic resonance imaging-based semiquantitative and quantitative assessment in osteoarthritis. Rheum. Dis. Clin. North Am. 35, 521–555.

Shenk, J.S., Workman, J., Westerhaus, M.O., 2001. Application of NIR spectroscopy to agricultural products. Pract. Spectrosc. 27, 419–474.

Siebelt, M., van Tiel, J., Waarsing, J.H., Piscaer, T.M., van Straten, M., Booij, R., Dijkshoorn, M.L., Kleinrensink, G.J., Verhaar, J.A., Krestin, G.P., Weinans, H., Oei, E.H., 2011a. Clinically applied CT arthrography to measure the sulphated glycosaminoglycan content of cartilage. Osteoarthritis Cartilage 19, 1183–1189.

Siebelt, M., Waarsing, J.H., Kops, N., Piscaer, T.M., Verhaar, J.A., Oei, E.H., Weinans, H., 2011b. Quantifying osteoarthritic cartilage changes accurately using in vivo microCT arthrography in three etiologically distinct rat models. J. Orthop. Res. 29, 1788–1794.

Siebert, F., 1995. Infrared spectroscopy applied to biochemical and biological problems. Methods Enzymol. 246, 501–526.

Spahn, G., Felmet, G., Baumgarten, G., Plettenberg, H., Hoffmann, M., Klinger, H., Hofmann, G., 2013a. Evaluation of cartilage degeneration by near infrared spectroscopy (NIRS): methodical description and systematic literature review. Z. Orthop. Unfall. 151, 31–37.

Spahn, G., Felmet, G., Hofmann, G.O., 2013b. Traumatic and degenerative cartilage lesions: arthroscopic differentiation using near-infrared spectroscopy (NIRS). Arch. Orthop. Trauma Surg. 133, 997–1002.

Spahn, G., Plettenberg, H., Kahl, E., Klinger, H.M., Muckley, T., Hofmann, G.O., 2007. Near-infrared (NIR) spectroscopy. A new method for arthroscopic evaluation of low grade degenerated cartilage lesions. Results of a pilot study. BMC Musculoskelet. Disord. 8, 47.

Spahn, G., Plettenberg, H., Nagel, H., Kahl, E., Klinger, H.M., Muckley, T., Gunther, M., Hofmann, G.O., Mollenhauer, J.A., 2008. Evaluation of cartilage defects with near-infrared spectroscopy (NIR): an ex vivo study. Med. Eng. Phys. 30, 285–292.

Squires, G.R., Okouneff, S., Ionescu, M., Poole, A.R., 2003. The pathobiology of focal lesion development in aging human articular cartilage and molecular matrix changes characteristic of osteoarthritis. Arthritis Rheum. 48, 1261–1270.

Sutter, R., Zubler, V., Hoffmann, A., Mamisch-Saupe, N., Dora, C., Kalberer, F., Zanetti, M., Hodler, J., Pfirrmann, C.W., 2014. Hip MRI: how useful is intraarticular contrast material for evaluating surgically proven lesions of the labrum and articular cartilage? AJ. Am. J. Roentgenol. 202, 160–169.

van der Rest, M., Garrone, R., 1991. Collagen family of proteins. FASEB J. 5, 2814–2823.

Venables, H.J., Wells, J.I., 2001. Powder mixing. Drug Dev. Ind. Pharm. 27, 599–612.

Venn, M., Maroudas, A., 1977. Chemical composition and swelling of normal and osteoarthrotic femoral head cartilage. I. Chemical composition. Ann. Rheum. Dis. 36, 121–129.

West, P.A., Bostrom, M.P., Torzilli, P.A., Camacho, N.P., 2004. Fourier transform infrared spectral analysis of degenerative cartilage: an infrared fiber optic probe and imaging study. Appl. Spectrosc. 58, 376–381.

Weyer, L., 1985. Near-infrared spectroscopy of organic substances. Appl. Spectrosc. Rev. 21, 1–43.

Williamson, A.K., Chen, A.C., Sah, R.L., 2001. Compressive properties and function–composition relationships of developing bovine articular cartilage. J. Orthop. Res. 19, 1113–1121.

Xia, Y., Ramakrishnan, N., Bidthanapally, A., 2007. The depth-dependent anisotropy of articular cartilage by Fourier-transform infrared imaging (FTIRI). Osteoarthritis Cartilage 15, 780–788.

Yin, J., Xia, Y., 2010. Macromolecular concentrations in bovine nasal cartilage by Fourier transform infrared imaging and principal component regression. Appl. Spectrosc. 64, 1199–1208.